Shale Oil Generation Conditions and Exploration Prospects of the Cretaceous Nenjiang Formation in the Changling Depression, Songliao Basin, China

Wenjun Zhang [1], Wenyu Zhang [2], Shumin Lin [1], Xing Ke [1], Min Zhang [1,*] and Taohua He [1]

[1] Hubei Key Laboratory of Petroleum Geochemistry and Environment, Yangtze University, Wuhan 430100, China; 329452627@163.com (W.Z.); 18299104807@163.com (S.L.); 15807288652@163.com (X.K.); hetaohua@yangtzeu.edu.cn (T.H.)

[2] SINOPEC Economics & Development Research Institute Company Limited, Beijing 100029, China; wenyu_zhang123@163.com

* Correspondence: zmjpu@163.com

Abstract: Low-maturity shale oil predominates in shale oil resources. China's onshore shale oil, particularly the Cretaceous Nenjiang Formation in the Songliao Basin, holds significant potential for low-maturity shale oil, presenting promising exploration and development prospects. This study delves into the hydrocarbon generation conditions, reservoir characteristics, and oil-bearing property analysis of the mud shale from the Nen-1 and Nen-2 sub-formations of the Nenjiang Formation to pinpoint favorable intervals for shale oil exploration. Through the integration of lithology, pressure, and fracture distribution data in the study area, favorable zones were delineated. The Nen-1 sub-formation is widely distributed in the Changling Depression, with mud shale thickness ranging from 30 to 100 m and a total organic content exceeding 2.0%. Type I kerogen predominated as the source rock, while some samples contained type II kerogen. Organic microcomponents primarily comprised algal bodies, with vitrinite reflectance (R_o) ranging from 0.5% to 0.8%. Compared to Nen-1 shale, Nen-2 shale exhibited less total organic content, kerogen type, and thermal evolution degree, albeit both are conducive to low-maturity shale oil generation. The Nen-1 and Nen-2 sub-formations predominantly consist of clay, quartz, feldspar, calcite, and pyrite minerals, with minor dolomite, siderite, and anhydrite. Hydrocarbons primarily reside in microfractures and micropores, including interlayer micropores, organic matter micropores, intra-cuticle micropores, and intercrystalline microporosity, with interlayer and intra-cuticle micropores being dominant. The free oil content (S_1) in Nen-1 shale ranged from 0.01 mg/g to 5.04 mg/g (average: 1.13 mg/g), while in Nen-2 shale, it ranged from 0.01 mg/g to 3.28 mg/g (average: 0.75 mg/g). The Nen-1 and Nen-2 sub-formations are identified as potential intervals for shale oil exploration. Considering total organic content, oil saturation, vitrinite reflectance, and shale formation thickness in the study area, the favorable zone for low-maturity shale oil generation is primarily situated in the Heidimiao Sub-Depression and its vicinity. The Nen-2 shale-oil-enriched zone is concentrated in the northwest part of the Heidimiao Sub-Depression, while the Nen-1 shale-oil-enriched zone lies in the northeast part.

Keywords: shale oil; hydrocarbon generation condition; Nenjiang Formation; Changling Depression; Songliao Basin

1. Introduction

With the remarkable success of unconventional oil and gas exploration and development, particularly in shale gas, shale oil has emerged as a focal point for global exploration efforts [1–10]. Studies on 158 oil-rich shale formations across 116 basins worldwide indicate approximately 251.2 billion tons of technically recoverable shale oil reserves, comprising 209.9 billion tons of low-maturity shale oil and 41.3 billion tons of medium–high maturity

shale oil [11–19]. This underscores the substantial resource potential and exploration opportunities associated with low-maturity shale oil. The continuous breakthrough of shale oil technology has played a supporting role in increasing and stabilizing the development of shale oil. The United States, with shale oil production reaching 376 million tons in 2019, constituting approximately 50% of the country's total crude oil production, has played a pivotal role in transforming the nation into a net crude exporter, thereby significantly impacting the global energy landscape [20]. China boasts abundant shale oil resources in onshore basins, with initial estimates suggesting recoverable shale oil resources ranging from 30 to 60 billion tons [21]. These resources are distributed widely across basins such as Songliao, Junggar, Ordos, and Bohai Bay [21–29]. Given China's substantial import dependence on foreign crude oil (71.06% in 2019), the development and utilization of shale oil and other unconventional resources are imperative for achieving energy independence and ensuring energy security [30–32].

Shale oil can be classified into low-maturity (<0.70% R_o) and medium–high maturity ($\geq$0.70% R_o) categories, with the former accounting for 60% to 70% of total shale oil resources in China [33]. Initial low production rates from most early-stage shale oil wells primarily stem from low oil maturity, high viscosity, high wax content, and poor fluidity [34]. However, the in situ conversion process (ICP), such as electrical heating, fluid heating, and radiation heating, can enhance oil recovery and render field development economically viable [35–37]. Shell's proposed in situ conversion process using electrical heating has been acknowledged as one of the most mature technologies for in situ shale oil extraction [38,39]. Hence, low-maturity shale oil holds the potential to revolutionize the oil and gas industry in China, sustaining long-term oil production at a scale of 2 million tons per year or even doubling the current production level [40].
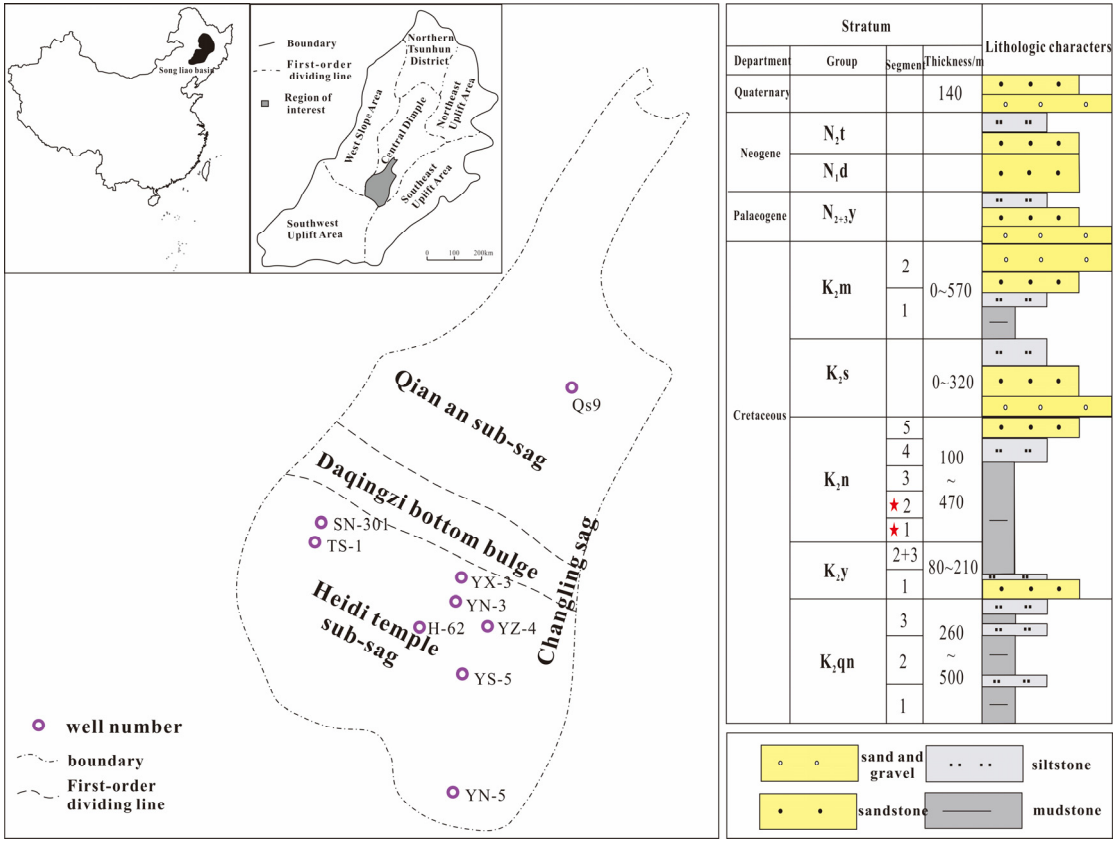
The Cretaceous Nenjiang Formation in the Songliao Basin harbors significant potential for low-maturity shale oil resources. Drilling outcomes from 109 wells targeting the Cretaceous Nenjiang Formation have revealed oil and gas discoveries, with several wells demonstrating industrial oil flow rates, indicating a favorable exploration outlook in the region and underscoring its importance for oil resource replacement [32,37]. Extensive research has been conducted to study the organic geochemical characteristics, shale oil enrichment mechanism, and paleo-environmental characteristics during shale deposition in the Nenjiang Formation of the Songliao Basin [41,42]. Additionally, simulation studies, such as those employing kinetic modeling of hydrocarbon generation and the thermal conduction models by Liu et al., have forecasted significant shale oil and gas resources in the Nenjiang Formation post in situ electrical heating [37]. These studies project a potential of 24.5 billion tons equivalent after five years of heating in the Nen-1 Sub-Formation and 6.59 billion tons equivalent for the Nen-2 Sub-Formation, indicating substantial oil and gas resource potential.

This research focuses on analyzing test results from 895 samples obtained from 69 different wells drilled at the Nenjiang Formation of the Changling Depression in the Songliao Basin. Of these samples, 482 are from the Nen-1 Sub-Formation and 413 are from the Nen-2 Sub-Formation. Through analyses of hydrocarbon generation conditions, reservoir characteristics, and oil-bearing properties in the shale formations of the Changling Depression, favorable exploration intervals have been identified. By integrating assessments of lithology, pressure, and fracture characteristics, favorable exploration areas have been delineated. This study significantly contributes to understanding shale oil exploration potential in low-thermal evolution basins, with both theoretical and practical implications.

2. Geological Background of Shale Oil Generation in the Songliao Basin

The Songliao Basin, situated in the northeastern region of China, spans across Heilongjiang, Jilin, and Liaoning provinces. It represents a rhombus-shaped basin covering an area of approximately 26,000 square kilometers, characterized as a significant Mesozoic–Cenozoic terrestrial sedimentary basin [43]. The Changling Depression, predominantly located in the southern part of the Songliao Basin (Figure 1), encompasses an area ex-

ceeding 20,000 square kilometers, exhibiting distinct structural attributes such as a fault–basin double-layer structure. The fault depression layers are primarily centered around deep-water faulted lacustrine sedimentation, characterized by rapid subsidence and the subsequent rapid infilling of over-compensation sedimentation. Tectonic fault activities significantly control sedimentation within this region. Additionally, influenced by the paleostructural background and sediment water dynamics, the southern segment of the Songliao Basin experiences overall regression from the Nen-1 Formation to the Ming-2 Formation. The facies transition trend from bottom to top comprises semi-deep lake to deep lake subfacies, shallow lake subfacies, delta front subfacies (braided river delta front subfacies), and delta plain subfacies (braided river delta plain subfacies). The depression layer exhibits a unified sedimentation area with extensive sedimentation coverage and stable sedimentation characteristics. The strata within the depression encompass the Lower Cretaceous Denglouku Formation, Quantou Formation (K_1q), Upper Cretaceous Qingshankou Formation (K_2qn), Yaojia Formation (K_2y), and Nenjiang Formation (K_2n) [44–46]. The Changling Depression comprises three tectonic units: the Heidimiao Subsag, Daqingzi Low Anticline, and Qian'an Subsag (Figure 1).

Figure 1. Structural unit and stratigraphic section of the Changling Sag in the Songliao Basin. The two pentagonal stars are the main layers of this study.

The Nenjiang Formation, situated within the depression structural layer, originated during the second expansion phase of the ancient Songliao Basin. The Nenjiang Formation is mainly in semi-deep lake-deep lake and shallow lake sediments, characterized by the extensive development of dark-colored mudstone [47]. The Nenjiang Formation can be subdivided into five sub-formations from bottom to top, with the Nen-1 Sub-Formation and the lower part of the Nen-2 Sub-Formation primarily composed of dark brown oil shale (Figure 1), representing the principal hydrocarbon source layers. The lower part of the Nen-2 Sub-Formation serves as the regional standard layer for the basin. Lithologically, there is a gradual transition to black-gray mudstone and gray muddy sandstone upwards, with

overall contacts with the underlying strata. The Heidimiao oil-rich layer, spanning from the Nen-3 to Nen-5 sub-formations, primarily comprises gray muddy sandstone, sandstone, and sporadic gray-green mudstone layers or interbedded sandstone and mudstone [48]. The anoxic and reducing environment is an important factor controlling the development of source rocks and the enrichment of organic matter. The ratio of redox-sensitive elements such as V/(V + Ni) and Th/U are used to judge whether the Nenjiang Formation is generally in a reducing environment. The process of organic carbon being oxidized and consumed in the anoxic and reducing environment is limited, which is conducive to the enrichment of organic carbon in shale [49,50].

3. Geologic Conditions for Shale Oil Generation

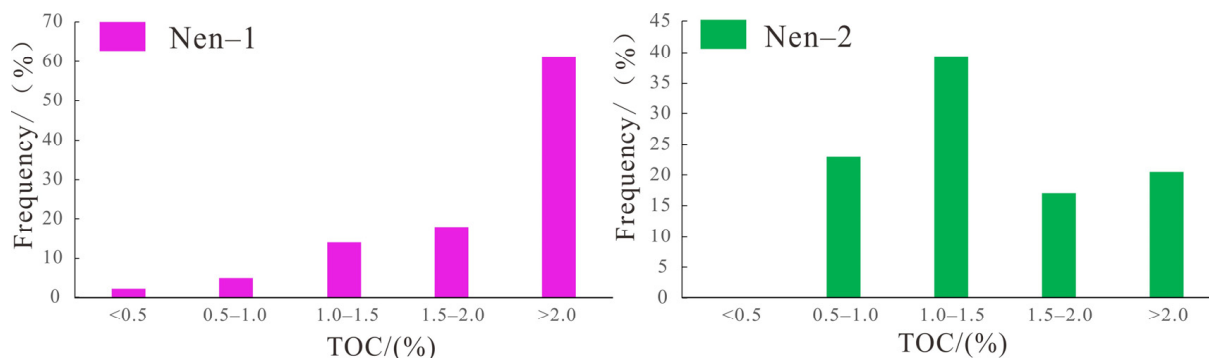### 3.1. Regional Distribution of Shale Formation

Organic-rich shale plays a pivotal role in shale oil generation and accumulation, with thickness and distribution range being critical factors in identifying favorable shale oil enrichment zones [51,52]. The Changling Depression experienced two significant black boom events during its depression stage, with the Qingshankou and Nenjiang formations exhibiting the widest lake basin coverage. These two lake transgression and regression cycles led to the formation of source rocks in the Qingshankou and Nenjiang formations. The warm and humid climate facilitated abundant aquatic and terrestrial vegetation, making these formations the primary shale development intervals in the Changling region [53–55]. The depth of oil- and gas-bearing shale in the Nen-1 Sub-Formation ranges from 500 m to 1900 m, gradually increasing from the periphery to the center of the depression. The thickness of oil- and gas-bearing shale varies from 30 m to 100 m, showing an increasing trend from the southwest source area to the northeast deep sag area. In the case of the Nen-2 Sub-Formation, the depth of the oil- and gas-bearing shale top ranges from 400 m to 1700 m, with increasing thickness from the surrounding areas toward the center of the sag. The thickness distribution of oil- and gas-bearing shale ranges between 30 m and 90 m, with thickness exceeding 80 m in the Qian'an–Daqingzi–Heidimiao area at the center of the depression. The thickness and burial depth of the Upper Cretaceous Nen-1 and Nen-2 shale formations meet the evaluation criteria for favorable shale oil zones, making them potential intervals for studying hydrocarbon generation and shale oil enrichment in the study area.

3.2. Hydrocarbon Generation Conditions in Shale Formations

The abundance of organic matter, type of organic matter, and thermal maturity are critical factors influencing the degree of oil and gas enrichment in shale formations. From the perspective of the Nenjiang Formation, the organic matter abundance of most shale samples is medium–good, the organic matter types are mainly Type I and Type II, the degree of thermal evolution is low, and the whole is in the low mature–mature stage.

3.2.1. Abundance of Organic Matter

The abundance of organic matter significantly impacts the intensity and quantity of hydrocarbon generation. Shale oil reservoirs with high production typically exhibit a total organic carbon (TOC) exceeding 2.0% [56]. The TOC range of the Nen-1 shale (238 samples) was from 0.06% to 8.37%, with an average of 2.68%. For the Nen-2 shale (171 samples), the TOC range was from 0.55% to 11.54%, with an average of 1.68%. The majority of Nen-1 shale samples had a TOC exceeding 2.0%, while Nen-2 shale samples predominantly exhibited TOC ranges between 1.0% and 1.5%. The chloroform asphalt 'A' value of hydrocarbon source rocks in the study area from the Nen-1 and Nen-2 sub-formations generally fell between 0.1% and 2.0%, indicating moderate to high levels of organic matter. Overall, the Nen-1 shale exhibited a higher abundance of organic matter compared to Nen-2 shale (Figure 2).

Figure 2. The TOC distribution frequency diagram of the Nen-1 and Nen-2 in the Changling Sag.

Using the rock pyrolysis analyzer, parameters such as free hydrocarbons and pyrolytic hydrocarbons can be obtained, and then the hydrocarbon generation capacity of source rocks can be evaluated. The sample was heated in a helium flow, and the free gaseous hydrocarbons, free liquid hydrocarbons, and pyrolytic hydrocarbons discharged from pyrolysis were detected by a hydrogen ion flame. The carbon dioxide discharged from pyrolysis and the carbon dioxide generated by heating and oxidizing the residual organic matter after pyrolysis were detected by a thermal conductivity detector. The relevant parameters of source rocks can be obtained, such as free hydrocarbon (S1), cracked hydrocarbon (S2), hydrocarbon generation potential (S1 + S2), and the highest pyrolysis peak (T_{max}) [57,58].

The 'A' values of chloroform bitumen in the source rocks of Nen-1 and Nen-2 in the study area were generally distributed between 0.1% and 2.0%, all of which were above medium. Among them, the 'A' value of chloroform asphalt in the tender section was between 0.231% and 1.429%, with an average of 0.678%. The 'A' value of chloroform asphalt in Nen-2 was between 0.068% and 1.164%, with an average of 0.289%. The total hydrocarbon content (HC) ranged from 1732 to 10,719 ppm, with an average of 5088 ppm. The total hydrocarbon content of the Nen-2 was between (512~5820) ppm, with an average of 2171 ppm.

The hydrocarbon generation potential ($S_1 + S_2$) of the Nen-1 was between 0.06 mg/g and 72.47 mg/g, with an average of 19.67 mg/g. Most of the samples were distributed in the range of 10 mg/g~20 mg/g, followed by more than 20 mg/g. The number of samples greater than 2.0 mg/g and 6.0 mg/g accounted for 98% and 82% of the total number of samples, respectively. The hydrocarbon generation potential of the Nen-2 was between 0.17 mg/g and 82.42 mg/g, with an average of 13.79 mg/g, and the hydrocarbon generation potential was slightly lower than that of the Nen-1.

From the total organic carbon, chloroform asphalt 'A', total hydrocarbon, $S_1 + S_2$, and other parameters, we found that the abundance of organic matter in the Nen-1 was higher.
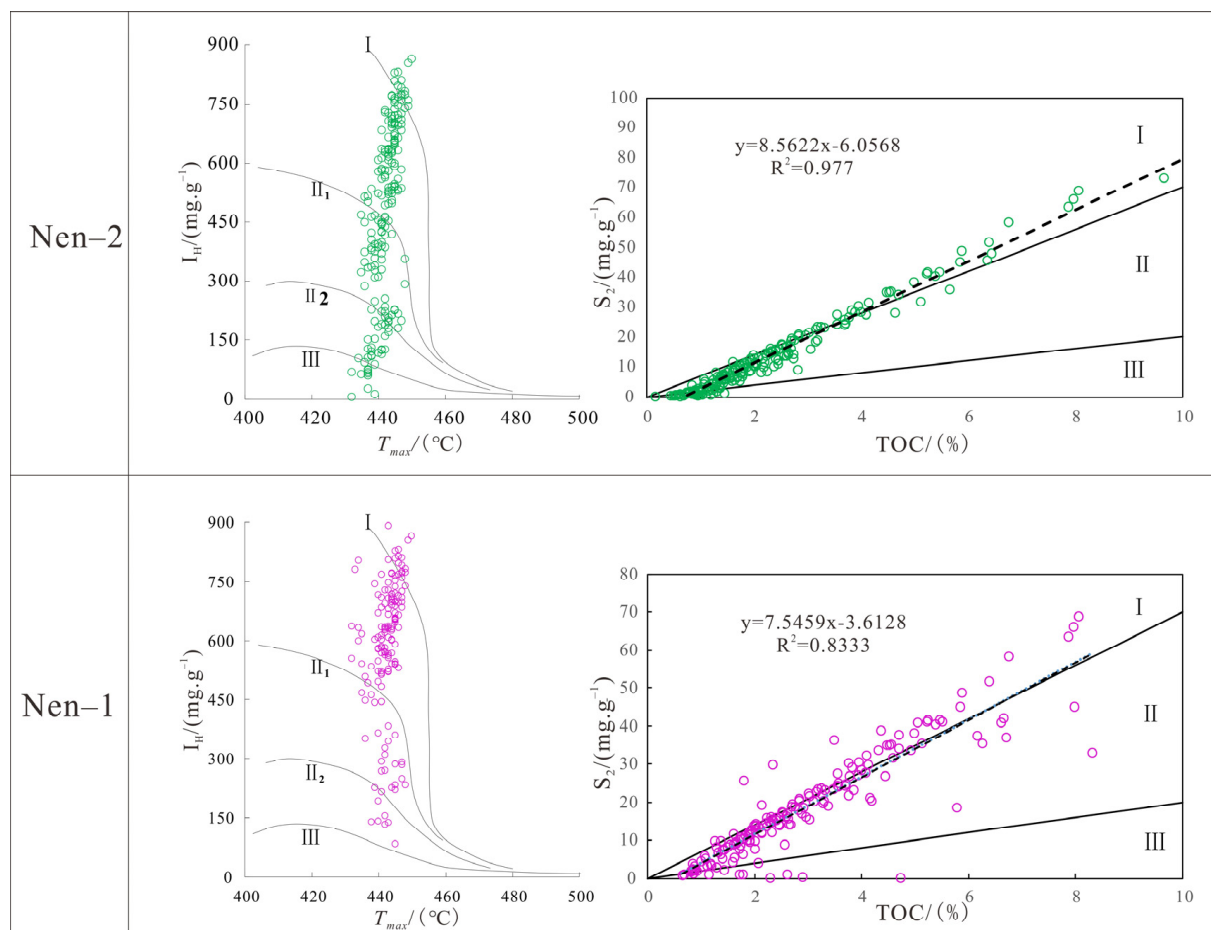
3.2.2. Types of Organic Matter

The type of organic matter significantly influences hydrocarbon generation potential. Type I and Type II kerogen are associated with oil generation, while Type III kerogen primarily generates gas [58]. Pyrolysis analysis on shale samples from the Upper Cretaceous Nenjiang Formation in the Changling Depression revealed that Nen-1 shale samples primarily contain Type I kerogen, with some samples containing Type II kerogen. In contrast, Nen-2 shale samples exhibit a variety of kerogen types, including sapropelic (Type I), humo-cambial (Type II$_1$), and sapropel-humo (Type II$_2$). However, the majority of Nen-2 samples belong to the sapropelic type (Type I–II$_2$).

The hydrogen index and oxygen index chart can effectively classify the types of organic matter. Type I organic matter produces a large amount of pyrolysis hydrocarbon S2 and poor carbon dioxide S3 during pyrolysis, while Type III organic matter only produces a small amount of heat transfer hydrocarbon and rich carbon dioxide S3 [57]. According

to the analysis of existing shale samples (Figure 3), the distribution range of pyrolysis hydrocarbon S_2 in the shale of the Nen-1 is between 0.05 and 68.8 mg/g, with an average of 18.54 mg/g. The actual hydrogen index obtained from the linear slope (R^2 = 0.83) of S_2 and TOC was found to be about 755 mg/g, indicating that the Nen-1 is mainly Type I~II$_1$ kerogen, which is consistent with the measured hydrogen index. The distribution range of pyrolysis hydrocarbon S_2 in the Nen-2 was 0.17 mg/g~82.42 mg/g, with an average of 13.79 mg/g. From the linear slope of S_2 and TOC (R^2 = 0.98), the actual hydrogen index was about 856 mg/g, revealing that the organic matter type of most samples is Type I~II$_2$ kerogen [59].

Figure 3. The division diagram of organic matter types in the Nen-1 and Nen-2 in the Changling Sag.
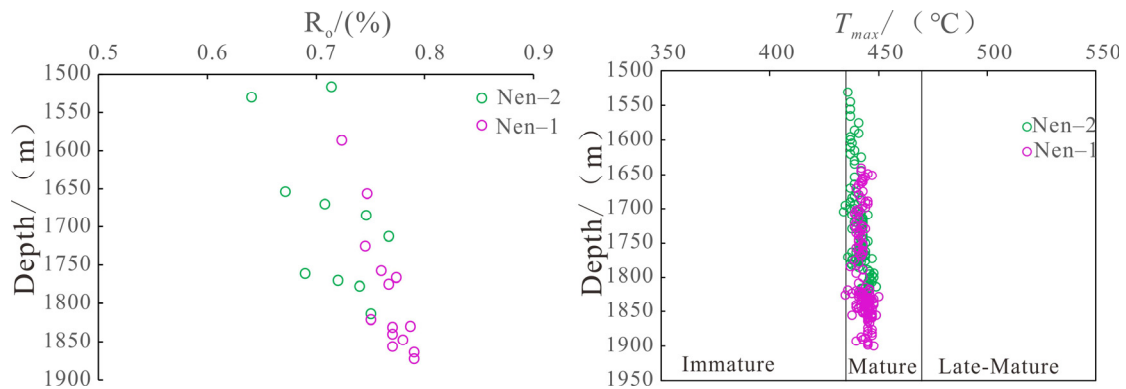
The macerals of typical samples show that the samples were mainly composed of the sapropel group, and the relative content of the components was between 44.9% and 96.5%, with an average of 80.9%. In a small amount of vitrinite, the relative content was between 4.5% and 16.7%, the average was 9.57%; the content of liptinite and inertinite was less. In general, the organic matter type of the sample was between Type I and Type II.

In summary, for the oil generation properties of shale in the Changling Sag, the organic matter type of the Nen-1 was better than that of the Nen-2, mainly Type II$_1$~I kerogen; the type of organic matter in the Nen-2 was mainly Type II$_2$~I.

3.2.3. Thermal Evolution

Vitrinite reflectance (R_o) is a crucial parameter for determining the thermal evolution stage of organic matter. The peak period of hydrocarbon generation is an important period for shale oil and gas accumulation. Many studies have shown that the maturity of organic matter R_o is generally 0.5%~1.2% [60,61]. The shale samples of the Nenjiang Formation
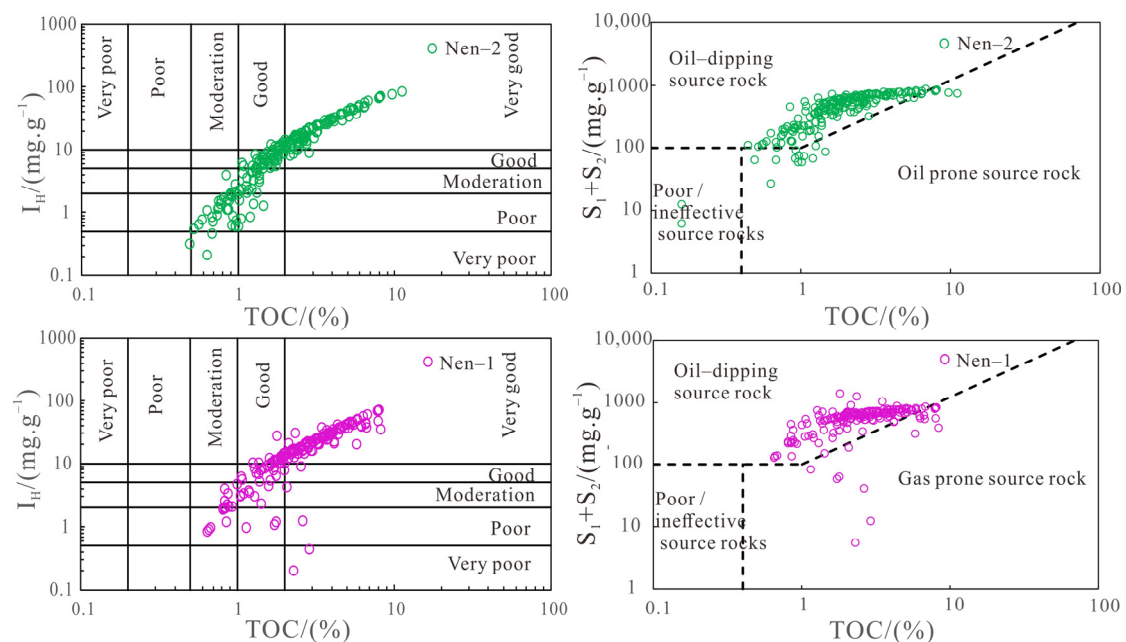
were distributed between 0.50% and 0.80%. Among them, the vitrinite reflectance R_o of the shale in the Nen-1 was distributed between 0.59% and 0.80%, which is in the stage of low-mature to mature thermal evolution. The vitrinite reflectance R_o of shale in the Nen-2 was between 0.58% and 0.77%, which is in the stage of low maturity to mature thermal evolution. The thermal evolution degree of Nen-1 shale was slightly higher than that of Nen-2 shale due to burial depth influence (Figure 4).

Figure 4. The relationship between R_o, T_{max}, and buried depth of the Nen-1 and Nen-2 in the Changling Sag.

3.2.4. Comprehensive Evaluation of Hydrocarbon Generation Potential

By combining TOC with the sum of S_1 and S_2 and intersecting TOC with the Hydrogen Index (IH), it can be concluded that shale samples from the Nenjiang Formation in the study area were predominantly oil-prone source rocks with high hydrocarbon generation capabilities (Figure 5). Nen-1 shale exhibited better-quality source rock compared to Nen-2 shale, particularly in terms of organic matter abundance. Nen-2 shale samples predominantly exhibited 'moderate' to 'good' quality, with fewer samples showing 'poor' quality, while Nen-1 shale samples mostly displayed 'good to very good' quality organic matter abundance, with fewer samples exhibiting 'poor' quality.
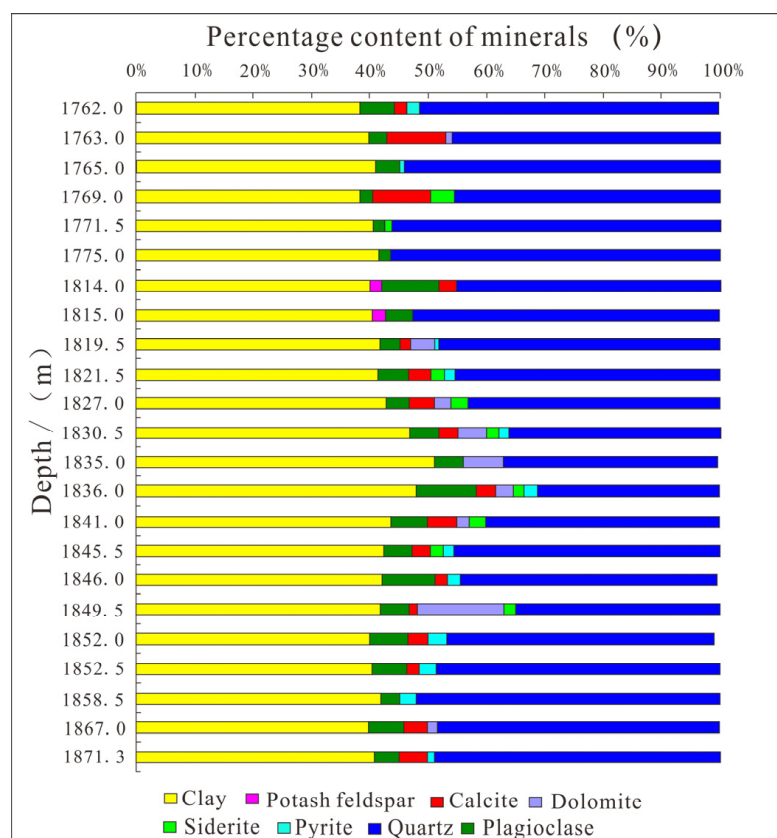

Figure 5. Comprehensive evaluation map of hydrocarbon generation potential and hydrocarbon generation tendency of the Nen-1 and Nen-2 in the Changling Sag, Songliao Basin.

3.3. Shale Reservoir Conditions

3.3.1. Mineral Composition

The rocks of the Nen-1 and Nen-2 sub-formations in the Changling Depression primarily consisted of clay minerals, quartz, feldspar, calcite, and pyrite, with minor amounts of dolomite, siderite, and anhydrite (Figure 6). The content of clay minerals ranged from 30.70% to 55.10%, while quartz content varied from 22.50% to 63.10%. Plagioclase feldspar content was generally low, ranging from 4.10% to 11.50%. Pyrite and calcite contents were both less than 5.60%, while dolomite can reach a maximum content of 29.90%.

Figure 6. Mineral composition content diagram of shale in the Nen-1 and Nen-2 in the Changling Depression (taking Yaonan 5 well as an example).

In the Nen-1 Sub-Formation, the mineral composition was dominated by clay minerals, quartz, and feldspar, with lower amounts of dolomite, calcite, pyrite, siderite, and gypsum. Clay minerals had the highest content, averaging 44.02%, followed by quartz with an average of 39.47%. Feldspar content averaged 6.31%, while carbonate mineral content averaged 7.51%. For the Nen-2 Sub-Formation, the mineral composition primarily comprised quartz, clay minerals, and feldspar, with small amounts of calcite, pyrite, siderite, and dolomite. Quartz had the highest content, averaging 52.00%, followed by clay minerals with an average of 38.46%. The average carbonate mineral content was 5.33%, with calcite averaging 2.54%.

3.3.2. Reservoir Space

The reservoir space of the Nen-1 and Nen-2 sub-formations in the Changling Depression was divided into two categories: fractures and pores, based on data such as core samples, thin sections, and scanning electron microscopy. The overall development of cracks was medium, mainly micro-cracks. There were four types of micropores developed in the pores: interlayer micropores, organic matter micropores, intra-debris micropores, and

intergranular micropores. Among them, interlayer micropores and intra-debris micropores were the main types of micropore development.

Fractures

The study area mainly consisted of mud with few clastic particles, characterized by moderately developed fractures, primarily microfractures. Some samples exhibited opened fractures with widths ranging from 4.093 μm to 181.82 μm, with the majority being larger than 20 μm. The average fracture width from all samples was 59.66 μm. Microfractures, with widths ranging from 0.40 μm to 18.18 μm, were also observed, with some being less than 10 μm. Overall, both open fractures and microfractures in the Nen-1 and Nen-2 sub-formations were moderately developed.

Pores

There are four types of pore development: interlayer micropores, organic matter micropores, bioclastic micropores, and intergranular micropores (Table 1). Among them, interlayer micropores and bioclastic micropores are the main types of micropore development.

Table 1. Micropore development types of shale in the Nenjiang Formation of the Changling Sag.
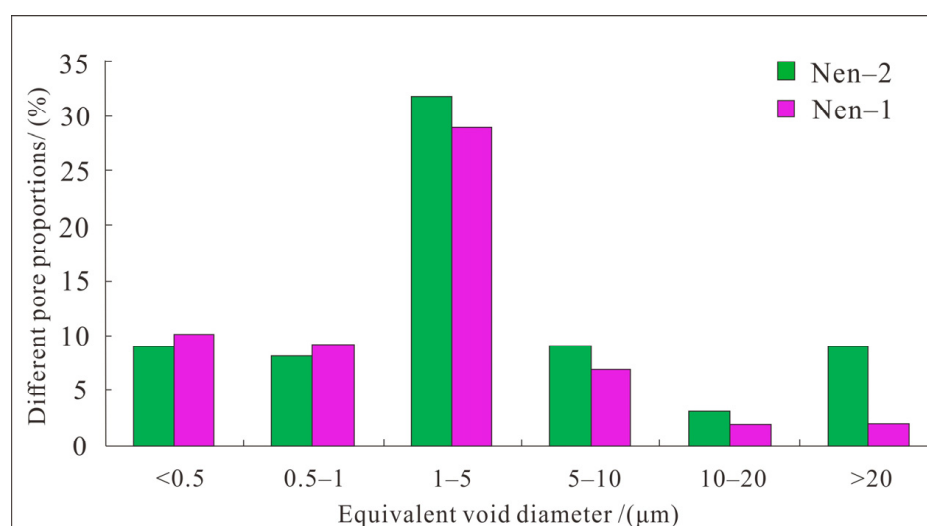
Micropore Type	Pore Carrier	Shape	Dimension	Relative Abundance	Connectivity
Interlayer microporosity	Illite/montmorillonite mixed interlayer	Spindle, ong strip, triangle	156.6 nm~5.6 μm	high	low
	Illite interlayer	Long strip, long form	1.81 μm~17.05 μm	low	mid
	Pyrite interlayer	Long strip	4.3 μm~40.3 μm	low	high
Organic microporosity	Organic matter itself	Long strip, fusiform	521.5 nm~9.18 μm	low	low
	Between organic matter and detrital structure	Long strip, oval	4.3 μm~11.96 μm	mid	mid
Micropores in biodebris	Higher plant debris	Roundness, long strip	262.7 nm~13.37 μm	mid	mid
	Animal debris	Long strip	101.5 nm~8.47 μm	mid	mid
	Cysts, spores	Bubble, irregular	638.8 nm~114.65 μm	high	mid
Intercrystalline micropore	Pyrite	Square, oval irregular	358 nm~9.19 μm	high	high
	Calcite	Oval, roundness	1 μm, 200 nm	low	low
	Gypsum	Long strip	2.6 μm	low	low

Interlayer micropores refer to the micropores generated by the bedding arrangement of minerals in rocks. There are three kinds of interlayer micropores (illite–montmorillonite mixed interlayer micropores, illite interlayer micropores, and banded mineral interlayer micropores). The morphology is mainly fusiform, long strip, and square. Among them are mainly developed illite–montmorillonite mixed interlayer mixed pores. The pore size of the micro-pores between illite–smectite mixed layers was between 156.6 nm and 5.6 μm, and 50% was concentrated between 1.0 μm and 4 μm. The pore size of the micro-pores between illite interlayers and pyrite interlayers was much larger than that of the micro-pores between illite–smectite mixed layers, up to 40.3 μm, but the abundance was very low.

Micropores in bioclastics refers to a series of debris formed by the collision between water flow and particles after the death of organisms, and then formed by diagenesis with sediments. The shale in the study area developed three kinds of micropores in the bioclast, which were mainly round, long strip, bubble, and irregular. Among them, the micropores in

the cysts were the most developed, and the pore size was between 638.8 nm and 114.65 μm. Most of them were micron-sized and mainly developed in the second section of the tender, and the micropores in the first section of the tender had a tendency to become smaller. The pore size of the second section of the micro-pore in the higher plant debris was obviously larger than that of the first section. The pore size of the micro-pore in the animal debris was between 101.5 nm and 8.47 μm, and some of them reached the nano-scale micro-pore with good connectivity.

The pore types developed in the study area mainly developed interlayer micropores, followed by intra-debris micropores, and the development of organic matter micropores and intergranular micropores was relatively small. From the frequency of the micro-pore diameter of the Nenjiang Formation, it is concluded that most of the micro-pore diameters developed in the Nen-1 and Nen-2 were less than 20 μm, concentrated with 1 μm~5 μm, and the pore widths of the Nen-2 were 1 μm~5 μm, 5 μm~10 μm, 10 μm~20 μm, >20 μm. The four levels were relatively larger than the Nen-1 (Figure 7). The average diameter of the Nen-2 was larger than that of the Nen-1, indicating that the micro-pores of the Nen-2 were more developed than the Nen-1.

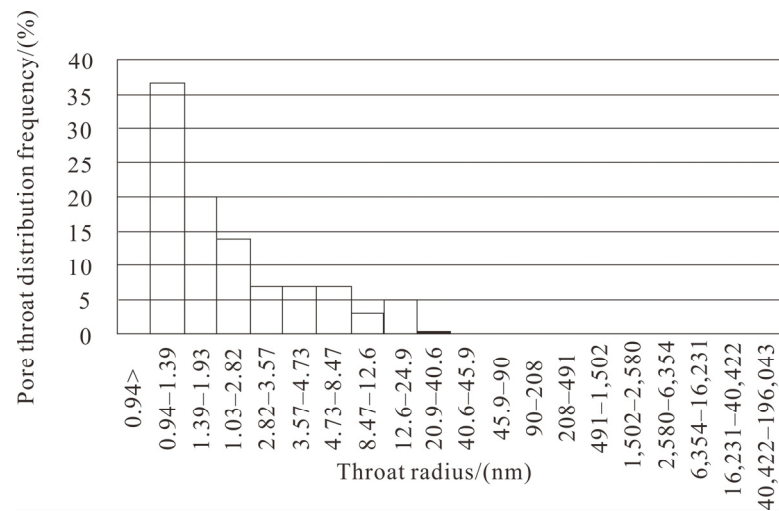**Figure 7.** Micropore diameter distribution map of the Nenjiang Formation in the Changling Sag.

Porosity of the Reservoir

It can be seen from Table 2 that the porosity of the Nen-2 (1764 m~1816 m) in Yaonan 5 well was 5.04%~10.91%, with an average value of 8.63%, and 1772 m reached 10.91%. The permeabilities of 1764 m and 1772 m were 0.000872 md and 0.000664 md, respectively, which belonged to medium-porosity to low-porosity and low-permeability to ultra-low-permeability reservoirs. The porosity of the first section (1818 m~1866 m) was 0.10%~4.40%, mostly concentrated at about 0.40%, and the porosity of 1858 m was only 0.14%. The permeabilities at 1850 m and 1866 m were 0.002370 md and 0.004270 md, respectively, which belonged to low-porosity to ultra-low-porosity and low-permeability reservoirs, but the porosity of the Nen-2 was significantly higher than that of the Nen-1.

The capillary pressure curve of shale in the Yaonan 5 well in the study area is characterized by fine skewness, fine throat, and poor throat sorting. It can be seen from Figure 8 that the breakthrough radius of the Yaonan 5 well was 5.000 nm~84.000 nm, and most of them were 5.000 nm~30.000 nm, indicating that the maximum pore throat radius of the Yaonan 5 well was 5.000 nm~30.000 nm. The median radius was 1.709 nm~9.165 nm, and most of them were located in 1.700 nm~2.5 nm, indicating that the pore throat concentration radius of the measured sample points in the Yaonan 5 well was 1.700 nm~2.500 nm.

Table 2. Shale porosity and permeability distribution table of the Yaonan 5 well.
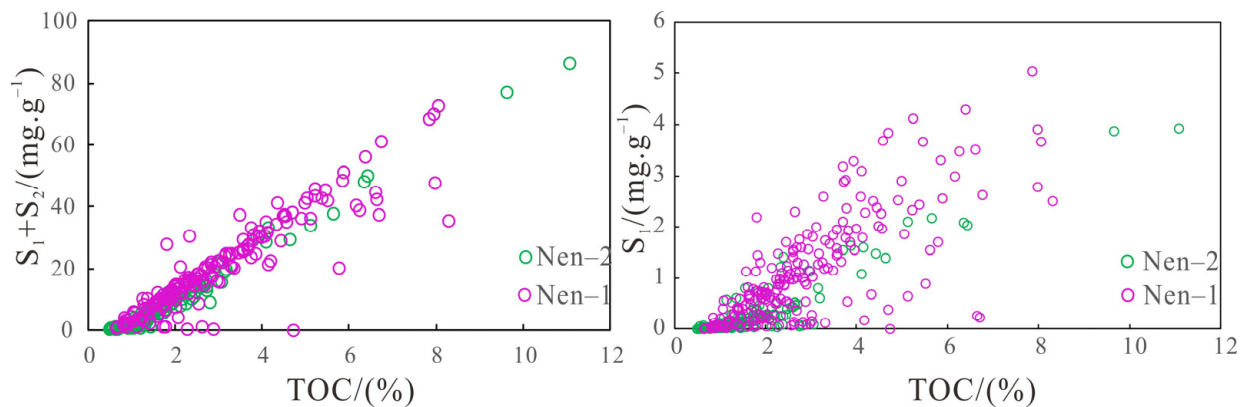
Layer	Depth (m)	Permeability (md)	Apparent Density (g/cm^3)	Porosity (%)
Nen 2	1764.00	0.000872	2.42	8.08
Nen 2	1768.00	/	2.35	9.63
Nen 2	1772.00	0.000664	2.36	10.91
Nen 2	1776.00	/	2.49	9.47
Nen 2	1816.00	/	2.40	5.04
Nen 1	1820.00	/	2.44	4.40
Nen 1	1824.00	/	2.36	0.51
Nen 1	1828.00	/	2.37	0.20
Nen 1	1834.00	/	2.37	0.32
Nen 1	1838.00	/	2.40	0.57
Nen 1	1842.00	/	2.38	0.40
Nen 1	1846.00	/	2.31	0.43
Nen 1	1850.00	0.002370	2.38	0.54
Nen 1	1854.00	/	2.32	0.21
Nen 1	1858.00	0.004270	2.33	0.14
Nen 1	1866.00	/	2.41	0.13

Figure 8. Distribution of the pore throat radius of the Nen 1 shale in the Yaonan 5 well of the Changling Sag, Songliao Basin.
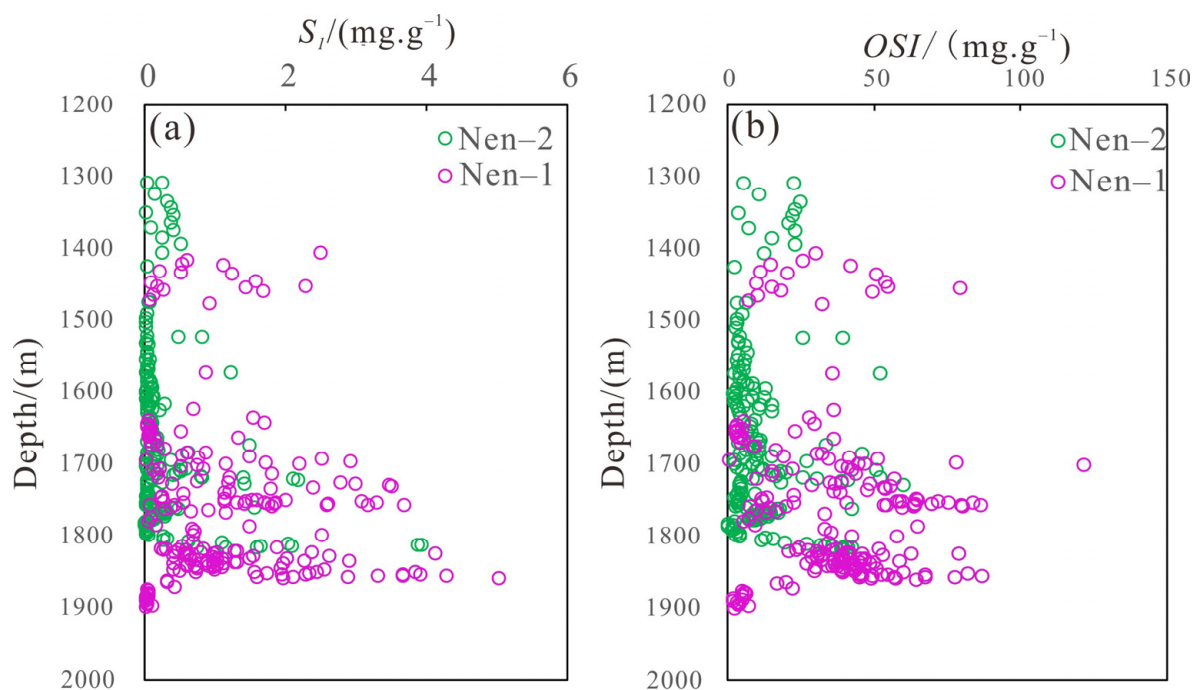
4. Assessment of Favorable Zones

4.1. Oil-Bearing Properties

The oil-bearing properties of shale, including adsorbed and free oil [9], are influenced by factors such as organic matter abundance and maturity. In the study area, most shale samples from the Nen-1 and Nen-2 sub-formations had a maturity ranging from 0.5% to 0.8%. The total retained oil content ($S_1 + S_2$) and free oil content (S_1) were positively correlated with total organic carbon (TOC) (Figure 9). Samples with a total retained oil content greater than 20 mg/g accounted for 70% of the total, while samples with an S1 content greater than 1.0 mg/g accounted for 60%.

Figure 9. The crossplot of source rocks ($S_1 + S_2$), S_1 and TOC in the Nen-1 and Nen-2 in the Changling Depression.

With increasing burial depth, the proportion of adsorbed oil decreased, while the amount of free oil increased (Figure 10a). The S1 distribution range for the Nen-2 samples was between 0.01 mg/g and 3.28 mg/g, with an average value of 0.75 mg/g, while for Nen-1 samples, it was between 0.01 mg/g and 5.04 mg/g, with an average value of 1.13 mg/g.

Figure 10. The variation trend of S_1 (**a**) and OSI (**b**) with depth in the Nen-1 and Nen-2 in the Changling Sag.

The Oil Saturation Index (OSI) [S1/TOC] exceeding 100 mg/g indicates the potential for a well-developed fractured shale oil reservoir, while an OSI between 75 mg/g and 100 mg/g suggests a potential shale oil reservoir [18]. After a burial depth of 1700 m, the S1 content significantly increased, indicating favorable conditions for the exploration of matrix-type shale oil reservoirs (Figure 10b). However, there were a few samples with an OSI greater than 75 mg/g. On the one hand, due to the long storage time of the analysis sample, the core was not cryopreserved on site. According to previous studies [7], the average loss rate of light hydrocarbons caused by conventional methods is 30% compared with that caused by liquid nitrogen freezing, and the average loss rate of light hydrocarbons is about 38% after the sample is placed for more than 54 h. Considering the influence of

the sample crushing method and storage time on light hydrocarbons, the free oil loss of conventional pyrolysis method is up to 50%. On the other hand, because the shale maturity of the Nen-1 and Nen-2 was not high as a whole, it did not reach the peak of oil generation. If the in situ heating transformation technology is adopted, it still has great shale oil exploration potential.

4.2. Favorable Stratigraphic Intervals

Based on comprehensive analysis, the Nen-1 Sub-Formation in the Changling Depression was identified as the most favorable shale oil interval. It exhibited high organic matter abundance (average TOC of 2.94%) and significant free oil content (average S_1 value of 1.13 mg/g). The presence of brittle minerals is also notable, with an average content of 48%. The natural gamma (GR) index is positively correlated with clay content and negatively correlated with brittle mineral content, which can reflect the distribution characteristics of brittle minerals on the plane from the side. The GR index of the Nenjiang Formation in the Longling Sag gradually increases from the southwest corner to the northeast corner. Combined with the geological background of the study area, it can be seen that the GR index gradually increases from the slope zone to the sag. The GR value of the Nen-1 in the study area was 95–125, and the GR value of the Nen-2 was between 90 and 105. The GR value of the Nen-1 was significantly higher than that of the Nen-2, indicating that the mud content of the Nen-1 was significantly higher than that of the Nen-2, and the overall evaluation was the best. The average TOC of the Nen-2 was 2.33%, the average S_1 was 0.75 mg/g, and the average brittle mineral content was 55%. The lithology was massive shale, lamina and micro-fractures were well developed, and the comprehensive evaluation was good.
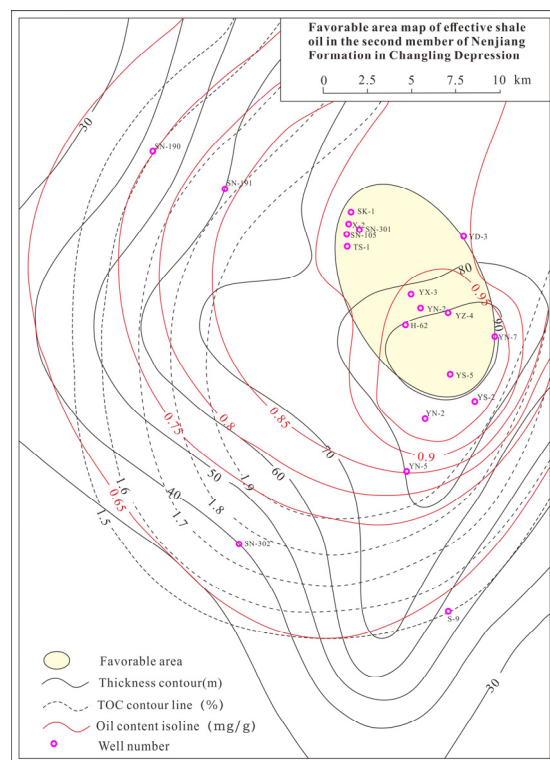
5. Favorable Zone Prediction

There are many geological factors to be considered in regional evaluation, including oil source conditions, reservoir conditions, cap rock conditions, trap conditions, preservation conditions, reservoir configuration conditions, and so on. In predicting favorable zones for shale oil exploration in the Changling Depression, several geological factors were considered, including total organic content (TOC), oil saturation (S_1), vitrinite reflectance, and shale thickness. Among these factors, TOC and oil saturation were deemed most crucial.
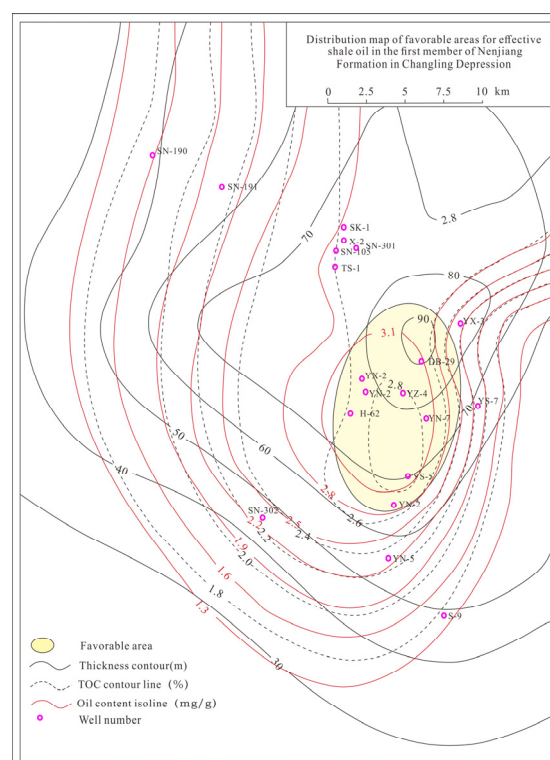
The high TOC, substantial effective shale thickness, and elevated oil saturation of the Nen-1 and Nen-2 sub-formations are primarily concentrated in the Haidimiao Sub-Depression and its adjacent areas. This indicates significant potential for exploring low-maturity shale oil in these regions. The thermal evolution degree of organic matter is generally low, suggesting that maturity has a limited impact on shale oil in the study area.

In summary, the favorable zone for the generation of low-maturity shale oil in the Changling Depression meets the criteria of TOC greater than 2.0%, effective shale thickness greater than 30 m, and oil saturation (S_1) greater than 0.5 mg/g. These zones are mainly concentrated in the Haidimiao Sub-Depression and its adjacent areas. Specifically, the favorable shale oil enrichment area in the Nen-2 Sub-Formation is located in the northwest part of the Haidimiao Sub-Depression (Figure 11), while in the Nen-1 Sub-Formation, it is situated in the northeast part of the Haidimiao Sub-Depression (Figure 12).

Figure 11. The favorable enrichment area of shale oil in the Nen-2 in the Changling Sag, Songliao Basin.

Figure 12. The favorable enrichment area of shale oil in the Nen-1 in the Changling Sag, Songliao Basin.

6. Conclusions

1. Through the analysis of TOC, free oil content (S_1), and hydrocarbon generation potential ($S_1 + S_2$), it was determined that the Nen-1 Sub-Formation in the Changling

Depression exhibits high organic matter abundance (TOC exceeding 2.0%) primarily composed of Type II$_1$–I kerogen, indicating mature thermal evolution. Through the systematic evaluation of organic matter abundance, type, and maturity, it is revealed that the Nen-1 has the greatest hydrocarbon generation potential. The TOC is greater than 2.0%, the organic matter type can easily generate oil, and the key shale layers in the maturity stage ($R_o > 0.7\%$) are mainly developed in the middle and top of the first and bottom of the Nen-2. This sub-formation demonstrates a high hydrocarbon generation potential, especially in its middle and bottom sections.

2. Mineral composition analysis revealed that the Nen-1 and Nen-2 sub-formations are primarily composed of clay, quartz, feldspar, calcite, and pyrite, with minor amounts of dolomite, siderite, and anhydrite. The micro-fractures of the shale in the study area are moderately developed, and four types of micro-pores are developed: interlayer micro-pores, organic micro-pores, intra-clast micro-pores, and inter-crystal micro-pores. Among them, interlayer micro-pores and intra-clast micro-pores are the main types of micro-pores. The porosity of the Nen-2 is obviously higher than that of the Nen-1, but the permeability is very low. From the four influencing factors of shale brittleness, quartz content, natural fracture, and diagenesis, the fracability coefficient of oil and gas shale rock in the Changling Sag is low, which belongs to medium fracability, and hydraulic fracturing can play a certain role.

3. The identified favorable zones for shale oil exploration are primarily located in the Heidimiao Sub-Depression and its surrounding areas. The favorable enrichment area of shale oil in the Nen-2 is concentrated in the northwest of the Heidimiao Sub-Sag, and the favorable enrichment area of shale oil in the Nen-1 is concentrated in the northeast of the Heidimiao Sub-Sag.

Author Contributions: W.Z. (Wenjun Zhang): conceptualization, methodology, writing, editing. W.Z. (Wenyu Zhang): data processing, experimental analysis, editing. S.L.: review, data processing. X.K.: data processing. M.Z.: conceptualization, review, and funding acquisition. T.H.: data processing. All authors have read and agreed to the published version of the manuscript.

Data Availability Statement: The data used to support the findings of this study are included within the article.

Conflicts of Interest: The Author Wenyu Zhang was employed by the SINOPEC Economics & Development Research Institute Company Limited. The remaining authors declare that the research was conducted in the absence of any commercial or financial relationships that could be construed as a potential conflict of interest.

References

1. Kinley, T.J.; Cook, L.W.; Breyer, J.A.; Jarvie, D.M.; Busbey, A.B. Hydrocarbon potential of the Barnett Shale (Mississippian), Delaware Basin, west Texas and southeastern New Mexico. *AAPG Bull.* **2008**, *92*, 967–991. [CrossRef]
2. Kuhn, P.P.; di Primio, R.; Hill, R.; Lawrence, J.R.; Hotsfield, B. Three-dimensional modeling study of the low-permeability petroleum system of the Bakken Formation. *AAPG Bull.* **2012**, *96*, 1867–1897. [CrossRef]
3. Jarvie, D.M. Shale resource systems for oil and gas: Part 2-Shale-oil resource systems. *AAPG Mem.* **2012**, *97*, 89–119.
4. Kirschbaum, M.A.; Mercier, T.J. Controls on the deposition and preservation of the Cretaceous Mowry Shale and Frontier Formation and equivalents, Rocky Mountain region, Colorado, Utah, and Wyoming. *AAPG Bull.* **2013**, *97*, 899–921. [CrossRef]
5. Zhang, M.; Li, H.B.; Wang, X. Geochemical characteristics and grouping of the crude oils in the Lishu fault depression, Songliao basin, NE China. *J. Pet. Sci. Eng.* **2013**, *110*, 32–39. [CrossRef]
6. Jiang, L.; Zhang, M. Geochemical characteristics and significances of rearranged hopanes in hydrocarbon source rocks, Songliao Basin, NE China. *J. Pet. Sci. Eng.* **2015**, *131*, 138–149. [CrossRef]
7. Wu, S.T.; Yang, Z.; Zhai, X.F.; Cui, J.W.; Bai, L.S.; Pan, S.Q.; Cui, J.G. An experimental study of organic matter, minerals and porosity evolution in shales within high-temperature and high-pressure constraints. *Mar. Pet. Geol.* **2019**, *102*, 377–390. [CrossRef]
8. Wang, C.; Zhang, B.Q.; Hu, Q.H.; Shu, Z.G.; Sun, M.D.; Bao, H. Laminae characteristics and influence on shale gas reservoir quality of lower Silurian Longmaxi Formation in the Jiaoshiba area of the Sichuan Basin, China. *Mar. Pet. Geol.* **2019**, *109*, 839–851. [CrossRef]

9. Atchley, S.C.; Crass, B.T.; Prince, K.C. The prediction of organic-rich reservoir facies within the Late Pennsylvanian Cline shale(also known as Wolfcamp D), Midland Basin, Texas. *AAPG Bull.* **2021**, *105*, 29–52. [CrossRef]

10. He, T.H.; Li, W.H.; Lu, S.F.; Yang, E.Q.; Jing, T.T.; Ying, J.F.; Zhu, P.F.; Wang, X.Z.; Pan, W.Q.; Chen, Z.H. Distribution and isotopic signature of 2-alkyl-1,3,4-trimethylbenzenes in the Lower Paleozoic source rocks and oils of Tarim Basin: Implications for the oil-source correlation. *Pet. Sci.* **2022**, *19*, 2572–2582. [CrossRef]

11. EIA. Technically Recoverable Shale Oil and Shale Gas Resources: An Assessment of 137 Shale Formations in 41 Countries Outside the United States. 2013. Available online: https://www.eia.gov/analysis/studies/worldshalegas/archive/2013/pdf/fullreport_2013.pdf?zscb=48295627 (accessed on 12 September 2024).

12. IHS. Unconventional Frontier: Prospects for Tight Oil in North America [EB/OL]. (2014-07-08) [2015-03-22]. Available online: http://www.ihs.com/products/cera/ (accessed on 12 September 2024).

13. Hartenergy. North American Shale Quarterly [EB/OL]. (2015-03-01) [2016-5-12]. Available online: https://www.hartenergy.com/ (accessed on 12 September 2024).

14. C&C. The Digital Analogs Knowledge System [DB/OL]. (2015-06-30) [2016-04-25]. Available online: https://ccreservoirs.com/daks/ (accessed on 12 September 2024).

15. IHS. Exploration, Production, and Midstream Information and Analysis Spanning over 250 Countries [EB/OL]. (2016-02-01) [2021-12-27]. Available online: https://my.ihs.com/Energy (accessed on 12 September 2024).

16. Jiang, L.; George, S.C.; Zhang, M. The occurrence and distribution of rearranged hopanes in crude oils from the Lishu Depression, Songliao Basin, China. *Org. Geochem.* **2018**, *115*, 205–219. [CrossRef]

17. Cheng, Q.S.; Zhang, M.; Li, H.B. Anomalous distribution of steranes in deep lacustrine facies low maturity-maturity source rocks and oil of Funing formation in Subei Basin. *J. Pet. Sci. Eng.* **2019**, *181*, 106190. [CrossRef]

18. Li, W.B.; Li, J.Q.; Lu, S.F.; Chen, G.H.; Pang, X.T.; Zhang, P.F.; He, T.H. Evaluation of gas-in-place content and gas-adsorbed ratio using carbon isotope fractionation model: A case study from Longmaxi shales in Sichuan Basin, China. *Int. J. Coal Geol.* **2022**, *249*, 103881. [CrossRef]

19. Zou, C.N.; Ma, F.; Pan, S.Q.; Zhang, X.S.; Wu, S.T.; Fu, G.Y.; Wang, H.J.; Yang, Z. Formation and distribution potential of global shale oil and the developments of continental shale oil theory and technology in China. *Earth Sci. Front.* **2023**, *30*, 128–142.

20. Ma, Y.S.; Cai, X.Y.; Zhao, P.R.; Hu, Z.Q.; Liu, H.M.; Gao, B.; Wang, W.Q.; Li, Z.M.; Zhang, Z.L. Geological characteristics and exploration practices of continental shale oil in China. *Acta Geol. Sin.* **2002**, *96*, 155–171.

21. Lu, S.F.; Huang, W.B.; Chen, F.W.; Li, J.J.; Wang, M.; Xue, H.T.; Wang, W.M.; Cai, X.Y. Classification and evaluation criteria of shale oil and gas resources: Discussion and application. *Pet. Explor. Dev.* **2012**, *39*, 249–256. [CrossRef]

22. Jia, C.Z.; Zheng, M.; Zhang, Y.F. Unconventional hydrocarbon resources in China and the prospect of exploration and development. *Pet. Explor. Dev.* **2012**, *39*, 129–136. [CrossRef]

23. Zou, C.N.; Yang, Z.; Zhu, R.K.; Zhang, G.S.; Hou, L.H.; Wu, S.T.; Tao, S.Z.; Yuan, X.J.; Dong, D.Z.; Wang, Y.M.; et al. Progress in China's unconventional oil & gas exploration and development and theoretical technologies. *Acta Geol. Sin.* **2015**, *89*, 979–1007.

24. Ning, F.; Wang, X.J.; Hao, X.F.; Zhu, D.Y.; Zhu, D.S. Division of Matrix-and Fracture-Type shale oils in the Jiyang depression and their differences. *Acta Geol. Sin. Engl. Ed.* **2015**, *89*, 1963–1972.

25. Kuang, L.C.; Hou, L.H.; Yang, Z.; Wu, S.T. Key parameters and methods of lacustrine shale oil reservoir characterization. *Acta Pet. Sin.* **2021**, *42*, 1–14.

26. Sun, L.D.; Liu, H.; He, W.Y.; Li, G.X.; Zhang, Y.C.; Zhu, R.K.; Jin, X.; Meng, S.W.; Jiang, H. An analysis of major scientific problems and research paths of Gulong shale oil in Daqing Oilfield, NE China. *Pet. Explor. Dev.* **2021**, *48*, 453–463. [CrossRef]

27. Fu, J.H.; Li, S.X.; Guo, Q.H.; Guo, W.; Zhou, X.P.; Liu, J.Y. Enrichment conditions and favorable area optimization of continental shale oil in Ordos Basin. *Acta Geol. Sin.* **2022**, *43*, 1702–1716.

28. He, W.Y.; Meng, Q.A.; Feng, Z.H.; Zhang, J.Y.; Wang, R. In-situ accumulation theory and exploration & development practice of Gulong shale oil in Songliao Basin. *Acta Pet. Sin.* **2022**, *43*, 1–14.

29. Li, G.X.; Zhu, R.K.; Zhang, Y.S.; Chen, D.; Cui, J.W.; Jiang, Y.H.; Wu, K.Y.; Sheng, J.; Xiang, C.G.; Liu, H. Geological characteristics, evaluation eriteria and discovery significance of Paleogene Yingxiongling shale oil in Qaidam Basin, NE China. *Pet. Explor. Dev.* **2022**, *49*, 18–31. [CrossRef]

30. Qian, X.K.; Liu, C.Q.; Jiang, X.F.; Xu, J.S.; Dai, J.Q. Overview of the domestic and foreign oil and gas industry development in 2019 and outlook for 2020. *Int. Pet. Econ.* **2020**, *28*, 2–9.

31. Zhao, W.Z.; Hu, S.Y.; Hou, L.H.; Yang, T.; Li, X.; Guo, B.C.; Yang, Z. Types and resource potential of continental shale oil in China and its boundary with tight oil. *Pet. Explor. Dev.* **2020**, *47*, 1–10. [CrossRef]

32. Zou, C.N.; Pan, S.Q.; Zhao, Q. On the connotation, challenge and significance of China's "energy independence" strategy. *Pet. Explor. Dev.* **2020**, *47*, 416–426. [CrossRef]

33. Li, M.W.; Jin, Z.J.; Dong, M.Z.; Ma, X.X.; Li, Z.M.; Jiang, Q.G.; Bao, Y.J.; Tao, G.L.; Qian, M.H.; Liu, P.; et al. Advances in the basic study of lacustrine shale evolution and shale oil accumulation. *Pet. Geol. Exp.* **2020**, *42*, 489–505.

34. Zhao, W.Z.; Hu, S.Y.; Hou, L.H. Connotation and strategic role of in-situ conversion processing of shale oil underground in the onshore China. *Pet. Explor. Dev.* **2018**, *45*, 537–545. [CrossRef]

35. Cui, J.W.; Zhu, R.K.; Hou, L.H.; Wu, S.T.; Mao, Z.G.; Li, S. Shale In-situ mining technology status quo of challenges and opportunities. *Unconv. Oil Gas* **2018**, *5*, 103–114.

36. Kang, Z.Q.; Zhao, Y.S.; Yang, D. Review of oil shale in-situ conversion technology. *Appl. Energy* **2020**, *269*, 115121. [CrossRef]

37. Liu, B.; Liu, Y.; Liu, Y.; He, J.L.; Gao, Y.F.; Wang, H.L.; Fan, J.; Fu, X.F. Prediction of low-maturity shale oil produced by in situ conversion: A case study of the first and second members of Nenjiang Formation in the central Depression, southern Songliao Basin, northeast China. *Pet. Geol. Exp.* **2020**, *42*, 533–544.

38. Fowler, T.D.; Vinegar, H.J. Oil shale ICP-Colorado field pilots. In Proceedings of the SPE Western Regional Meeting, San Jose, CA, USA, 24–26 March 2009.

39. Leverette, H.M. Status and plans for the U.S. department of interior program for development of oil shale and oil sands. In Proceedings of the 31st Oil Shale Symposium, Golden, CO, USA, 17–21 October 2011.

40. Lu, S.F.; Wang, J.; Li, W.B.; Cao, Y.X.; Chen, F.W.; Li, J.J.; Xue, H.T.; Wang, M. Economic feasibility and efficiency enhancement approaches for in situ upgrading of low-maturity organic-rich shale from an energy consumption ratio perspective. *Earth Sci. Front.* **2023**, *30*, 281–295.

41. Jia, J.L.; Bechtel, A.; Liu, Z.J.; Strobl, S.A.I.; Sun, P.C.; Sachsenhofer, R.F. Oil shale formation in the Upper Cretaceous Nenjiang Formation of the Songliao Basin (NE China): Implications from organic and inorganic geochemical analyses. *Int. J. Coal Geol.* **2013**, *113*, 11–26. [CrossRef]

42. Liu, B.; Song, Y.; Ye, X.; Zhu, K.; Yan, M.; Li, W.; Li, C.; Li, Z.H.; Tian, W.C. Algal-microbial community, paleoenvironment, and shale oil potential of lacustrine organic-rich shale in the Upper Cretaceous Nenjiang Formation of the southern central Depression, Songliao Basin (NE China). *ACS Earth Space Chem.* **2021**, *5*, 2957–2969. [CrossRef]

43. Xie, T. Study on Micropore Characteristics and Controlling Factors of Cretaceous Qingshankou Formation Shale in Songliao Basin. Master's Thesis, China University of Geosciences (Beijing), Beijing, China, 2020.

44. Feng, Z.; Huo, Q.L.; Wang, X.; Zeng, H.S.; Fu, L. Organic geochemical characteristics and paleosedimetary environments of the source rocks in member 1 of Qingshankou formation. *Pet. Geol. Oilfield Dev. Daqing* **2015**, *34*, 1–7.

45. Zhang, D.Q. Study on Hydrocarbon Accumulation Conditions of Upper Cretaceous Nenjiang Formation in Chang-Ling Depression, Southern Songliao Basin. Master's Thesis, Jilin University, Changchun, China, 2018.

46. Li, L. Study on Shale Reservoir Characteristics of the First Member of Qingshankou Formation in Changling Sag, Southern Songliao Basin. Master's Thesis, Jilin University, Changchun, China, 2022.

47. He, B.Y.; Cui, W.B.; Zhang, J.Y. Geological characteristics and exploration breakthroughs of the middle to low mature shale oil of Nenjiang Formation in northern Songliao Basin. *Acta Pet. Sin.* **2024**, *45*, 900–913.

48. Mao, J.L.; Jing, T.Y.; Han, X.; Shang, C.; Huang, S.Q.; Ma, M.X. Petrology types and organic geochemical characteristics of shale in the Western Depression, Liaohe. *Earth Sci. Front.* **2016**, *23*, 185–194.

49. He, L. *Organic Matter Enrichment and Evolution of Sedimentary Environment of the Wufeng-Longmaxi Shale in Southeastern Margins of the Sichuan Basin*; Guangzhou Institute of Geochemistry, Chinese Academy of Sciences: Guangzhou, China, 2020.

50. Cui, H.S.; Guo, W.; Zhao, X.B.; Lin, B.; Wang, S.H. Sedimentary geochemical response of paleoenvironment of Nenjiang Formation in southeastern uplift of Songliao Basin. In Proceedings of the 14th Annual Meeting of Chinese Society of Mineral and Rock Geochemistry, Nanjing, China, 21–25 April 2013.

51. Zhang, J.C.; Jin, Z.J.; Yuan, M.S. Reservoiring mechanism of shale gas and its distribution. *Nat. Gas Ind.* **2004**, *24*, 15–18.

52. Yang, A.R.; Jia, Y.Y.; Tan, J.J.; Huang, Q.; Yi, A.; Yu, Z.Y. Research on continental shale oil forming conditions and exploration potential analysis in Nanyang depression. *Pet. Geol. Eng.* **2013**, *27*, 8–11.

53. Wang, Y.M.; Xiong, Y.Q.; Wang, L.W.; Miao, H.B. Hydrogen isotopic compositions of n-alkanes in crude oils and extracts of Upper Cretaceous from southern Songliao Basin. *Geochimica* **2006**, *35*, 602–608.

54. Zhu, J.X.; Zhang, X.W.; Luo, X.; Jia, Y.Y.; Dan, L.; Wu, Y.B. Continental shale oil resources and favorable area evaluation of Biyang depression. *Pet. Geol. Eng.* **2015**, *29*, 38–41.

55. Qin, M.H.; Wang, Z.P. Optimization of the favorable area and analysis of the resource potential for the upper cretaceous shale oil in Changling Depression, Songliao Basin. *Sci. Technol. Eng.* **2014**, *14*, 209–215.

56. Zou, C.; Yang, Z.; Cui, J.W.; Zhu, R.K.; Hou, L.H.; Tao, S.Z.; Yuan, X.J.; Wu, S.T.; Lin, S.H.; Wang, L.; et al. Formation mechanism, geological characteristics and development strategy of nonmarine shale oil in China. *Pet. Explor. Dev.* **2013**, *40*, 14–26. [CrossRef]

57. Wu, L.Y. *Rapid Quantitative Evaluation of Oil Rock Pyrolysis*; Science Press: Beijing, China, 1986.

58. Tissot, B.P.; Welte, D.H. *Petroleum Formation and Occurrence*; Springer: Berlin/Heidelberg, Germany, 1978.

59. Wang, X.; Liu, Y.H.; Zhang, M.; Hu, S.Y.; Liu, H.J. Conditions of Formation and Accumulation for Shale Gas. *Nat. Gas Geosci.* **2010**, *21*, 351–355.

60. Xiao, X.M.; Song, Z.G.; Zhu, Y.M.; Tian, H.; Yi, H.W. Summary of shale gas research in North American and revelations to shale gas exploration of Lower Paleozoic strata in China south area. *J. China Coal Soc.* **2013**, *38*, 721–727.

61. Zhang, J.C.; Lin, L.M.; Li, Y.X.; Tang, X.; Zhu, L.L.; Xing, Y.W.; Jiang, S.L.; Jing, T.Y.; Yang, S.Y. Classification and evaluation of shale oil. *Earth Sci. Front.* **2012**, *19*, 322–331.